Engineered Science

RESEARCH PAPER

View Article Online

Remarkably Enhanced CO_2 Uptake and Uranium Extraction by Functionalization of Cyano-bearing Conjugated Porous Polycarbazoles

Anwang Dong,[1] Yaqi Zhu,[1] Mengyao Ren,[1] Xiaoyu Sun,[1] Vignesh Murugadoss,[3,4] Yihui Yuan,[1] Jun Wen,[2] Xiaolin Wang,[2] Qi Chen,[1*] Zhanhu Guo[3*] and Ning Wang[1*]

Cyano-bearing conjugated polycarbazoles PHN-1 and PHN-2 were efficiently prepared in high yields from corresponding monomers with para- and meta-configuration by oxidative coupling polymerization at room temperature, respectively. PHN-1 with para-configuration exhibits higher porosity than meta-configuration counterpart PHN-2. Cyano groups in the polymers were further converted to conjugated polycarbazoles containing tetrazole (PHN-1-TZ and PHN-2-TZ) or amidoxime groups (PHN-1-AO and PHN-2-AO) after treatment with NaN_3/NH_4Cl_3 and hydroxylamine aqueous solution, respectively. Up to 55.0% enhancement of CO_2 uptake at 298 K and 1.0 bar found for PHN-2-TZ (4.93 wt%) after post-modification from PHN-2 (3.18 wt%) is ascribed to tetrazole groups with basic feature and acidic hydrogen, which show high affinities to CO_2 not only by the Lewis acid–Lewis base and local-dipole-quadrupole interactions but also through the hydrogen bonding with oxygen atoms of CO_2. In the real seawater with excess uranium (8.02 ppm), a maximum uranium extraction uptake of 119.4 mg g^{-1} for PHN-1-AO greatly higher than ~10 mg g^{-1} for the PHN-1 (about) at room temperature is due to the strong chelating interaction between the amidoxime groups and uranium.

Keywords: Microporous polymers; Polycarbazoles; Modification; CO_2 uptake; Uranium extraction

Received 28 December 2018**, Accepted** 27 January2019

DOI: 10.30919/es8d688

1. Introduction

As one of the conjugated microporous polymers (CMPs), porous conjugated polycarbazoles by coupling of π-conjugated building blocks containing carbazole moieties not only exhibit rich electronic properties and high porosities, but also retain particular functions derived from relevant monomers.[1] Their structures are diverse due to the existence of various π-conjugated building blocks such as arenes, macrocycles and heterocyclic aromatic units as well as multiplicity of synthetic reactions such as classic C–C cross-coupling reactions,[2,3] oxidative coupling reaction[4,5] and electrochemical polymerization.[6-8] Porous polycarbazoles with high Brunauer–Emmett–Teller (BET) specific surface area up to 2400 m^2 g^{-1} possess stable pore structure and narrow pore size distribution (PSD) at 0.6–2.5 nm.[1] Their cooptoelectronic application is very broad raning from conjugated detection system[3] and organic electronic devices,[6,7] to electrochemical reduction of CO_2[9] and the photocatalysts.[10] Therefore, the intrinsic porosities and optoelectronic properties as well as chemical and thermal stability led to increasing interests and extensive researches in synthetic strategies, preparative methods, and functionalization.[11,12]

The ever-growing anthropogenic carbon dioxide (CO_2) emissions have caused many environmental problems and attracted growing attention nowadays.[13-19] Both CO_2 and methane are greenhouse gases and can along with water to form gas hydrate.[20-24] The combustion of fossil fuels in power plants is the main reason for the increased CO_2 emissions.[25-27] The exploitation of carbon capture and storage (CCS) materials and the development of new energy sources, such as nuclear energy,[28,29] are demanded urgently.[30-32] The nitrogen-containing porous polycarbazoles prepared by oxidative coupling reaction show potential advantages, such as low-cost preparation, good recyclability and high affinity with CO_2 and can be used as alternative CCS adsorbents.[33-37] For instance, the CO_2 absorption capacity of polycarbazole CPOP-9 (Carbazole-based Porous Organic Polymers, CPOPs) is high up to 70 wt% at 18.0 bar and 298 K.[34] Porous polycarbazoles CPOP-1 and P-PCz-3 also exhibit high CO_2 uptake of 21.2 and 25.3 wt%, respectively, at 1.0 bar and 273 K.[4,36]

On the other hand, only uranium reservoir sufficiency can warrant the continuous supply of nuclear energy.[38-40] Considering most of uranium is present in the seawater at the concentration of 3–3.3 ppb,[41-43] and the nuclear effluent with radioactive uranium from the nuclear industry which has great harm to humans and the environment,[44,45] to explore the adsorbent with strong adsorption capacity for uranium becomes demanding.[46,47] Various materials such as porous aromatic frameworks (PAFs),[41,48] CMPs,[49] metal-organic frameworks (MOFs),[50-52] hyper-cross-linked polymers,[53] molecularly imprinted polymers and inorganic materials[54,55] have been reported as the adsorbent for uranium. Among them, amidoxime-based porous materials are the most promising ones due to the high chelation between the amidoxime

[1] *State Key Laboratory of Marine Resource Utilization in South China Sea, Hainan University,Haikou 570228, China*

[2] *Institute of Nuclear Physics and Chemistry, China Academy of Engineering Physics, Mianyang 621900, China*

[3] *Integrated Composites Laboratory (ICL), Department of Chemcial & Biomolecular Engineering, University of Tennessee, Knoxville TN 37996, USA*

[4] *Electro-Materials Research Laboratory, Centre for Nanoscience and Technology, Pondicherry University, Puducherry 605014, India*

***E-mail:** chenqi@hainu.edu.cn; zguo10@utk.edu; wangn02@foxmail.com*

© Engineered Science Publisher LLC 2019

groups and uranium.[56,57] Up to now, conjugated porous polycarbazoles with amidoxime groups have not been reported or used for the uranium extration.

For porous polymers, post-modification based on original polymers such as covalent graft or non-covalent coordination is useful to develop the materials with novel functions and applications.[58-62] For example, PAF-1 was covalently functionalized with thioether groups for selective copper capture and applied for detecting Wilson's disease.[63] Palladium complex can be coordinated into porous polycarbazole containing pyridine to fabricate the Pd-metalated nanoporous catalysts for the heterogeneous additive-free cyanation.[64] Inspired by high binding ability of nitrogen-rich organic porous materials to CO_2 and strong chelation of uranium with amidoxime-containing materials, herein, porous polycarbazoles containing cyano groups were prepared via $FeCl_3$-catalyzed oxidative coupling reaction. Through post-polymerization modification, porous polycarbazoles containing tetrazolyl or amidoxime groups were prepared and studied for CO_2 adsorption, and uranium extraction from simulated seawater with different uranium concentrations and the real seawater with excess uranium.

2. Experimental Section

2.1 Materials

Hydroxylamine aqueous solution (50%) was bought from Alfa Aesar Co., Ltd. Carbazole, uranyl nitrate hexahydrate, iron (III) chloride, potassium tert-butoxide, 4-fluorobenzaldehyde, sodium methoxide, sodium hydroxide and ammonium chloride were ordered from Macklin Co., Ltd. Potassium carbonate, 1,3-phenylenediacetonitrile and 1,4-phenylenediacetonitrile were purchased from Aladdin Reagent Co., Ltd. Sea salt was purchased from Yier Be Co., Ltd. The common solvents such as methanol, tetrahydrofuran (THF), *N*, *N*-Dimethylformamide (DMF), and dichloromethane (DCM) were commercially available from Xilong Co., Ltd. The real seawater is obtained from Wanning nearby the south china sea. All the chemicals and solvents were used as received. 4-(9-Carbazolyl)benzaldehyde was tailored via an previous method.[65]

2.2 Characterization and measurement

The content of this part is in the supporting information.

2.3 Preparation of monomers and polymers

*Synthesis of Monomers **M-1** and **M-2***: Under the continuous magnetic stirring, 1,4-phenylenediacetonitrile (50 mg, 0.32 mmol) and 4-(9-carbazolyl)benzaldehyde (170 mg, 0.63 mmol) were dissolved completely in THF (5.0 mL) at room temperature. Sodium methoxide (50 mg, 0.92 mmol) in methanol (5.0 mL) was added dropwise to the mixture. A yellow solid was precipitated in 5 min, and 20 min later, the mixture of concentrated hydrochloric acid (0.5 mL) and methanol (20 mL) was added dropwise to stop the reaction. After filtration and repeated washing by ethanol, the monomer **M-1** was obtained as a mixture of isomers after drying in vacuum (190 mg, 89.3%) without further purification. ^{1}H NMR (400 MHz, $CDCl_3$, δ): 8.20 (d, 4H, *J* = 8.8 Hz), 8.17 (d, 4H, *J* = 7.6 Hz), 7.87 (s, 4H), 7.75 (d, 4H, *J* = 8.4 Hz), 7.74 (s, 2H), 7.74 (d, 4H, *J* = 8.0 Hz), 7.46 (t, 4H, *J* = 7.8 Hz), 7.34 (t, 4H, *J* = 6.8 Hz); ^{13}C NMR (100 MHz, $CDCl_3$, δ): 143.9, 142.0, 140.4, 140.3, 140.2, 139.7, 135.6, 133.8, 132.2, 132.1, 132.0, 131.6, 131.2, 130.0, 127.2, 127.0, 126.9, 126.4, 126.3, 124.0, 123.9, 120.8, 120.7, 119.9, 117.8, 113.9, 111.1, 110.0, 109.9; MS (APCI-TOF) m/z [M]: calculated for $C_{48}H_{30}N_4$, 662.73; found, 662.25.

According to similar synthetic procedures to **M-1**, monomer **M-2** was synthesized from 1,3-phenylenediacetonitrile (50 mg, 0.32 mmol) and 4-(9-carbazolyl) benzaldehyde (170 mg, 0.63 mmol) to afford a pure yellow solid (175 mg, 82.2%). ^{1}H NMR (400 MHz, $CDCl_3$, δ): 8.21 (d, 4H, *J* = 8.4 Hz), 8.17 (d, 4H, *J* = 7.6 Hz), 8.04 (s, 1H), 7.81 (dd, 2H, *J* = 8.0, 2.0 Hz), 7.78 (s, 2H), 7.75 (d, 4H, *J* = 2.8 Hz), 7.63 (t, 1H, *J* = 7.6 Hz), 7.54 (d, 4H, *J* = 8.4 Hz), 7.46 (t, 4H, *J* = 7.2 Hz), 7.34 (t, 4H, *J* = 6.8 Hz). ^{13}C NMR (100 MHz, $CDCl_3$, δ): 142.4, 140.4, 140.2, 135.7, 132.1, 131.3, 127.2, 126.4, 124.0, 120.8, 120.7, 118.0, 111.3, 110.0; MS (APCI-TOF) m/z [M]: calculated for $C_{48}H_{30}N_4$, 662.73; found, 662.24.

*Preparation of polymers **PHN-1** and **PHN-2***: To a round-bottomed flask, iron (III) chloride (245 mg, 0.91 mmol) and anhydrous DCM (5.0 mL) were added at room temperature. **M-1** (100 mg, 0.15 mmol) completely dissolved in anhydrous DCM (10 mL) was injected into the suspension successively and stirred overnight. The entire reaction system was continuously protected with argon and completely excluded from oxygen until the reaction was completed. After the reaction was finished, anhydrous methanol was added and stirred for 30 minutes to dissolve iron (III) chloride. The undissolved solid was washed repeatedly by three varying organic solvents and water. Finally, after Soxhlet extraction with methanol and THF for 24 h, respectively, polymer **PHN-1** was obtained as a brick-red powder (97 mg, 97.0%) with drying for 12 h.

According to similar synthetic procedures to polymer **PHN-1**, **PHN-2** was prepared from monomer **M-2** (100 mg, 0.15 mmol) to afford a yellowish solid (95 mg, 95.0%).

*Preparation of polymers **PHN-1-TZ** and **PHN-2-TZ***: Under argon atmosphere, **PHN-1** (200 mg, 0.30 mmol, calculated based on the repeating unite) was dispersed in anhydrous DMF (20 mL) with magnetic stirring for 30 min. To the solution, ammonium chloride (321 mg, 6.00 mmol) and sodium azide (390 mg, 6.00 mmol) were added at the same time. The resulting suspension was stirred at 120 °C under the argon protection for 3 days. After being cooled down to room temperature, the dilute hydrochloric acid (70 mL, 0.25 mol L^{-1}) was added dropwise to precipitate the solid product completely. The mixture was centrifugated and washed by water several times to obtain polymer **PHN-1-TZ** (204 mg, 90.5%) after the Soxhlet extraction with methanol and THF for 24 h and drying in vacuum.

According to similar synthetic procedures to polymer **PHN-1-TZ**, **PHN-2-TZ** was prepared from the parent polymer **PHN-2** (200 mg) to afford a yellowish solid (210 mg, 93.2%).

*Preparation of Polymers **PHN-1-AO** and **PHN-2-AO***: Under magnetic stirring, **PHN-1** (100 mg, 0.15 mmol), anhydrous potassium carbonate (100 mg, 0.72 mmol) and hydroxylamine aqueous solution (5.0 mL) were dissolved or dispersed in alcohol (20 mL) at 70 °C for 2 d. After being cooled down to room temperature, the suspension mixture was filtered and washed by ultrapure water, methanol, DCM and THF repeatedly. Finally, a light yellow solid **PHN-1-AO** (105 mg, 92.2%) was produced after Soxhlet extracts with methanol for 12 h and drying in vacuum for 24 h.

According to similar synthetic procedures to polymer **PHN-1-AO**, **PHN-2-AO** was prepared from parent polymer **PHN-2** (100 mg, 0.15 mmol) to afford a light yellow solid (107 mg, 94.0%).

2.4 Uranium extraction tests

Uranium uptake studies in simulated seawater: All the uranium solutions (500 ml) with different uranium concentrations (i.e., 10, 20, 30, and 40 ppm) were obtained via the adjustment of different uranyl nitrate hexahydrate and sea salt (16.7 mg). The pH of uranium solution was modulated at 7.5 by hydrochloric acid or sodium hydroxide before the measurement. All the uranium uptake tests of the prepared polymers

© Engineered Science Publisher LLC 2019

were carried out according to the same procedures. For instance, **PHN-1-AO** (5.0 mg) and uranium solution (500 mL, 10 ppm, pH 7.5) were added in the plastic bottle and were placed in a constant rocking shaker at the speed of 100 rpm. At intervals of 2 h, aliquots (5.0 mL) of the sample were separated from the mixture and filtered through syringe membrane filter (0.45 μm). The uranium concentration in the resulting solutions and uranium uptake were analyzed quantitatively via the reported method.[41]

Uranium uptake studies in real seawater with excess uranium: The real seawater with excess uranium was prepared by the addition of uranyl nitrate hexahydrate in the filtered real seawater (500 mL). The prepared polymer adsorbent (5.0 mg) and the real seawater with excess uranium (500 mL, 8.02 ppm) were added in the plastic bottle and were placed in a constant rocking shaker at the speed of 100 rpm. The uptake capacity of the adsorbent for uranium in real seawater with excess uranium was tested by the same method in simulated seawater.[41] The adsorbent **PHN-1-AO** was eluted with sodium hydroxide solution (1.0 M) in its regeneration reseacrh.

3. Results and Discussion

3.1 Preparation and characterization

Synthesis routes to the monomers and polymers are shown in Scheme 1. The carbazole derivative 4-(9-carbazolyl)benzaldehyde was chosen as the starting material to prepare monomers at room temperature. The obtained material was coupled with phenylenediacetonitriles through the Knoevenagel condensation[66,67] to obtain monomers **M-1** and **M-2** in high yields efficiently. The monomers containing cyano groups can be synthesized quickly under the basic condition in 30 mins at room temperature without using the poisonous chemical reagents such as NaCN or CuCN,[41,50] which are usually used to prepare cyano-containing small molecules. The successful preparation of monomers **M-1** and **M-2** has been confirmed by ^{1}HNMR, ^{13}CNMR and MS (see Supporting Information), which indicate that monomer **M-1** is a mixture of isomers and monomer, while **M-2** is a pure compound. Based on our and others previous work,[1,34,68-73] oxidative coupling polymerization was selected to economically prepare conjugated polycarbazoles **PHN-1** and **PHN-2** from the corresponding monomers catalyzed by the low-cost and non-toxic catalyst $FeCl_3$ in high yields at room temperature. Given that no special functional group but carbazole involved in this polymerization, the cyano groups in **PHN-1** and **PHN-2** were completely preserved. The **PHN-1** and **PHN-2** were further modificated by NaN_3 and NH_4Cl at 120 °C to convert cyano groups to tetrazoles via [2+3] cycloaddition reaction,[74] and the corresponding **PHN-1-TZ** and **PHN-2-TZ** with tetrazoles were obtained. Besides, amidoxime-modificated **PHN-1-AO** and **PHN-2-AO** were also prepared by treatment **PHN-1** or **PHN-2** with hydroxylamine reagents. Hydroxylamine hydrochloride was firstly tried with K_2CO_3, however, most of cyano groups could not be converted to amidoxime groups. Finally, excessive hydroxylamine aqueous solution (50%) was used to push and complete this difficult heterogeneous transformation. All the prepared polymers were also well characterized.

From the (CP/MAS) NMR spectra of **PHN-1** and **PHN-2** (Fig. 1a), the observed chemical shifts and signal intensities of the polymers are consistent with the ^{13}CNMR spectra of the corresponding monomers. Generally, the observed distinctly four broad peaks with different chemical shifts (about 140, 125, 120 and 110 ppm) are similar to the reported data of other porous conjugated polycarbazoles.[4,33,34] The assignment of resonance peaks and detailed explanation of (CP/MAS) NMR spectra of **PHN-1** can be found in supporting information (Fig. S1). Post-modification of cyano-bearing polymers **PHN-1** and **PHN-2** can be verified clearly by FTIR spectra shown in Figs. S2 and 1b. For example, the FTIR spectrum of **PHN-2** shows the characteristic vibration absorption peak of cyano groups at 2215 cm^{-1} (Fig. 1b).[41] After modification of **PNH-2** to **PNH-2-TZ**, the signal peak of -C≡N at 2215 cm^{-1} of **PNH-2-TZ** becomes much weaker and the appearance of a new absorption peak at 1650 cm^{-1} is ascribed to the C=N- stretching vibration derived from the tetrazole ring of **PHN-2-TZ**. Moreover, a new absorption peak at about 3380 cm^{-1} is attributed to the stretching vibration of N-H in the tetrazole ring.[74] When **PHN-2** was converted to **PNH-2-AO**, the disappearance of the signal peak of -C≡N at 2215 cm^{-1} and a new absorption peak of -C=N- at 1658 cm^{-1} were found for the FTIR spectrum of **PHN-2-AO**.[41] The strong absorption peaks at about

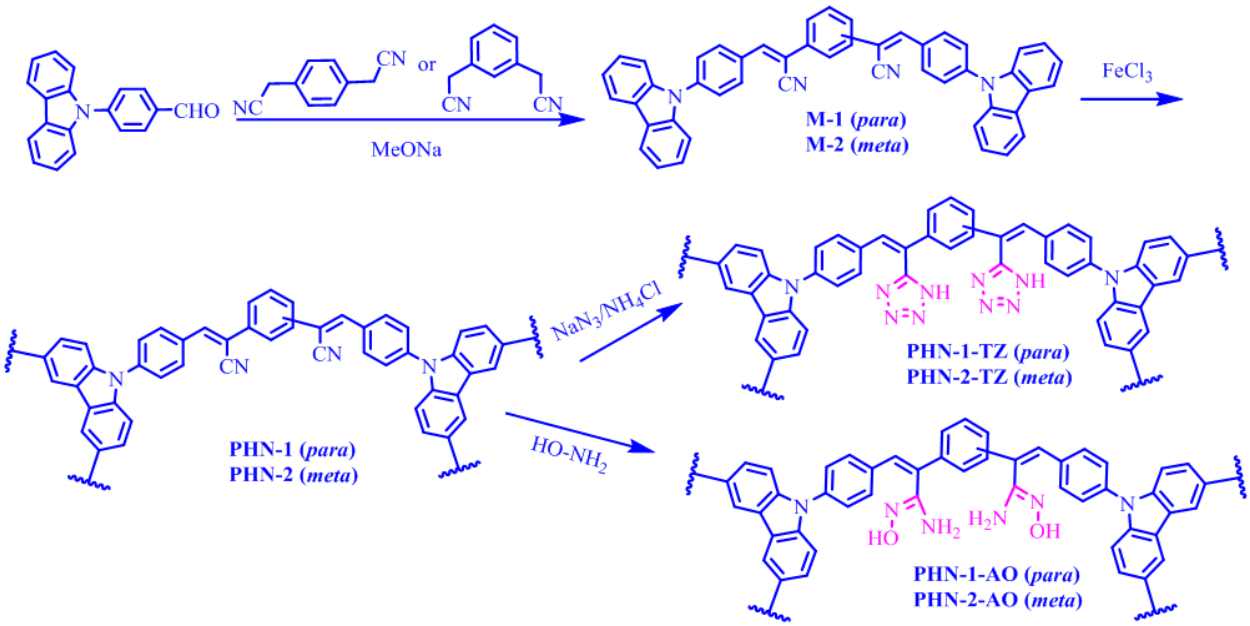

Scheme 1 Synthesis routes to the monomers and polymers.

© Engineered Science Publisher LLC 2019

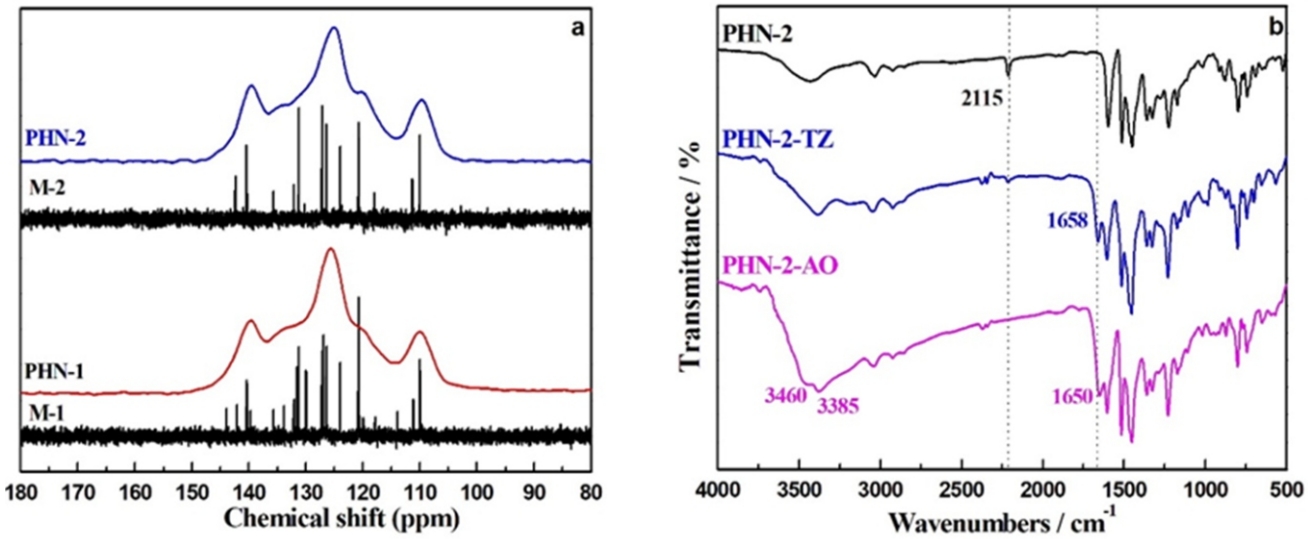

Fig. 1 (a) ^{13}C NMR spectra of **M-1**, **M-2**, **PHN-1**, and **PHN-2**. **(b)** FTIR spectra of the polymers **PHN-2**, **PHN-2-TZ**, and **PHN-2-AO**.

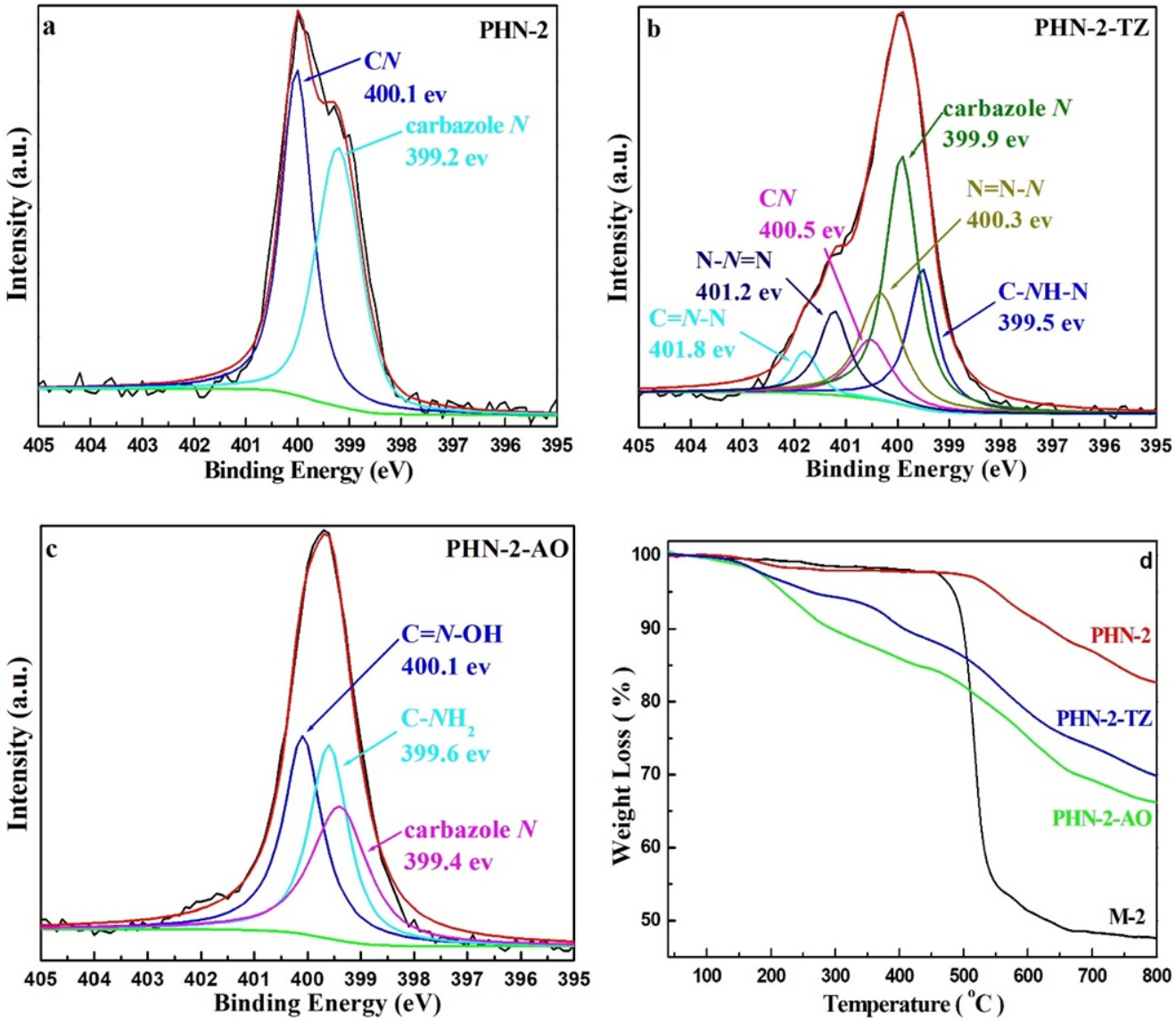

Fig. 2 N1s XPS data (a, b, c) and TGA plots (d) under N_2 atmosphere of **PHN-2**, **PHN-2-TZ**, and **PHN-2-AO**.

© Engineered Science Publisher LLC 2019

3460 and 3385 cm^{-1} also respond to the -NH_2 and -OH groups derived from the amidoxime groups in **PHN-2-AO**.[51,54]

To further prove the successful post-modification, XPS data of nitrogen species of the six polymers were investigated. As shown in Fig. 2a, the N 1s peak of PHN-2 is composed of the nitrogen in *N*-phenyl carbazoles and the nitrogen of cyano groups with the bonding energy of 399.2 and 400.0 eV, respectively. After being converted to **PNH-2-TZ**, its N 1s peak was located at the higher binding energy (Fig. 2b) and divided into six different nitrogen signal peaks including -C-*N*H- (399.5 eV), *N*-phenyl carbazole (399.9 eV), -C=*N*-N (401.8 eV), the residuary -C≡*N* ≡*N*(400.3 eV), -N-*N*=N (401.2 eV), and N=*N*-N= (400.5 eV), individually.[75] For **PHN-2-AO**, the N 1s XPS data (Fig. 2c) indicate three different N signals derived from *N*-phenyl carbazole (399.4 eV), =*N*-OH (400.1 eV) and -*N*H_2 (399.6 eV), respectively. Similar results were found for the XPS data of nitrogen species in the polymers **PHN-1, PNH-1-TZ** and **PHN-1-AO** (Fig.s S3a-c).

Thermal stability of the prepared monomers and polymers were studied by TGA in the N_2 atmosphere. The corresponding plots are shown in Fig.s 2d and S4. Monomers **M-1** and **M-2** show a 5% mass loss at about 490 °C and appears 52% mass loss at around 800 °C. After polymerization, the obtained polymers such as **PHN-2** exhibit higher decomposition temperature at about 550 °C and much lower mass loss (about 18%) at around 800 °C (Fig. 2d), which imply the successful polymerization. Post-modification from **PHN-2** to **PHN-2-TZ** or **PHN-2-AO** results in a decreased decomposition temperature at about 200 °C.[76] However, their mass loss at around 800 °C is still less than 35% due to the cross-linking nature, which is also the reason that all the prepared polymers are insoluble in common organic solvents, even in dilute acid and alkali aqueous solution. Microscopic structure of **PHN-1** and **PHN-2** were observed by SEM, as shown in the Fig.s S5a-b, both of them are composed of irregular aggregated particles similar to most of porous polycarbazoles reported before.[4,33,34]

3.2 Porosities

Nitrogen adsorption–desorption isotherms at 77 K were measured to analyze the porosities of all the polymers. As shown in Fig.s 3a and 3b, all polymers have the sharp rise in N_2 adsorption at a very low relative pressure (< 0.01), which indicates the existence of microporous substructure.[13,77] **PHN-1** and **PHN-2** have deep rise N_2 uptake at a high relative pressure (> 0.9), demonstrating the presence of macroporous

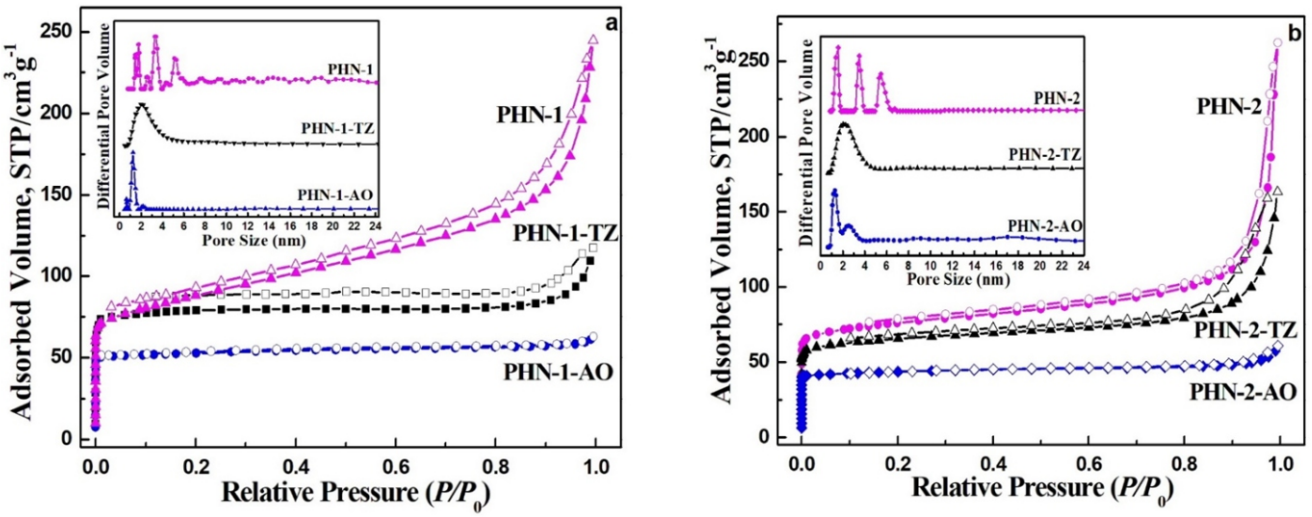

Fig. 3 Nitrogen adsorption–desorption isotherms of all prepared polymers (a and b) measured at 77 K and their PSD profiles calculated by NLDFT (inset). The adsorption and desorption branches are labeled with solid and open symbols, respectively.

Table 1 Porosities and CO_2 uptake capacities of polymers.

Polymers	S_{BET} [a] ($m^2\ g^{-1}$)	V_{total} [b] ($cm^3\ g^{-1}$)	D_{pore} [c] (nm)	CO_2 uptake [d] (wt%)
PHN-1	340	0.20	1.74, 3.31	4.13
PHN-2	293	0.15	1.52, 3.44	3.18
PHN-1-TZ	262	0.11	1.95	4.87 (6.96) [e]
PHN-2-TZ	235	0.09	2.10	4.93 (6.12) [e]
PHN-1-AO	206	0.08	1.25	-
PHN-2-AO	184	0.07	1.24	-

[a] Specific surface area calculated from the nitrogen adsorption isotherm using the BET method. [b] Total pore volume at P/P_0=0.99. [c] Date calculated from nitrogen adsorption isotherms with the NLDFT method. [d] Date were obtained at 1.0 bar and 298 K. [e] Date were obtained at 1.0 bar and 273 K.

© Engineered Science Publisher LLC 2019

structure. In addition, for **PHN-1**, **PHN-2**, **PHN-1-TZ**, and **PHN-2-TZ**, the appearance of hysteresis loops between the adsorption and desorption curves manifests that the pore width has some mesoporous distribution. As to **PHN-1-AO** and **PHN-2-AO**, their isotherms exhibit type I nitrogen sorption isotherms according to the IUPAC classification,[78] since the nitrogen adsorption increases slowly with the increase of the relative pressure, even in a high relative pressure (> 0.9).[79,80] The BET specific surface area (S_{BET}) values of **PHN-1** and **PHN-2** are 340 and 293 $m^2 g^1$, severally. Post-modification from **PHN-1** and **PHN-2** to the polymers containing tetrazoles (**PHN-1-TZ** and **PHN-2-TZ**) or amidoxime groups (**PHN-1-AO** and **PHN-2-AO**) gives rise to a decreased S_{BET}, which is in the range from 262 to 184 $m^2 g^1$. The corresponding PSD profiles of all polymers are shown in the insets of Figs. 3a and 3b. The dominant pore size of **PHN-1** is mainly centered at 1.74 and 3.2 nm. After modification, the dominant pore sizes of **PHN-1-TZ** and **PHN-1-AO** are decreased to about 1.95 and 1.25 nm, respectively. Similar PSD change tendency is found for the polymers **PHN-2**, **PHN-2-TZ** and **PHN-2-AO**. The key parameters of polymers porosity derived from their adsorption isotherms are shown in Table 1.

3.3 CO_2 uptake and uranium extraction performance

The cyano-bearing conjugated porous polycarbazoles are suitable matrix to produce functional porous polymers by the corresponding post-modification, which was used to endow the materials with different specific functions to solve the environment problem caused by CO_2 emisions stemed from the burning of fossil fuel in the power plants,[81-83] and the shortage of raw material uranium as well as the leakage of extremely radioactive and highly toxic radionuclide in utilization of nuclear energy,[38-45] individually.

As we know, nitrogen-rich organic porous materials especially porous polymers based on *N*-heterocycles such as pyridine,[36] carbazole4[33,34] and tetrazole[74] exhibit high binding abilities to CO_2 due to the Lewis acid–Lewis base interactions as well as the local-dipole-quadrupole interactions between the matrix and polarizable CO_2 molecules induced by high charge density of the nitrogen sites.[4] Tetrazole group with *pK*a about 4.89 possesses basic feature and acidic hydrogen, which show high affinities to CO_2 not only by the interactions mentioned above but also through the hydrogen bonding with oxygen atoms of CO_2.[74] Therefore, the modification of cyano groups into tetrazole groups is expected to improve the uptake capacities of porous polycarbazoles for CO_2 more than other gases. Uptake behavior of the related polymers for CO_2 was measured at 298 K under low pressure. Based on the carbon dioxide physisorption isotherms of polymers shown in Fig.s 4a and 4b, as expected, tetrazole-modified polymers **PHN-1-TZ** and **PHN-2-TZ** with a lower BET specific surface area exhibit higher CO_2 uptake capacities than corresponding parent polymers, individually. To our surprise, up to 55.0% enhancement of CO_2 uptake was found for **PHN-2-TZ** (4.93 wt%) after post-modification from **PHN-2** (3.18 wt%) at 298 K and 1.0 bar. This indicates that the incorporation of the tetrazole groups into porous polymers greatly promoted the CO_2 adsorption performance. At the conditions of 273 K and 1.0 bar, **PHN-1-TZ** and **PHN-2-TZ** show higher uptake capacities about 6.96 wt% and 6.12 wt%, respectively (Fig. S6).

The CO_2 uptake capacity of polymers **PHN-1-TZ** and **PHN-2-TZ** was enhanced apparently when the pressure was higher than 0.8 bar. Probably, the conformation changes of the polymer due to the rotation and stretching of randomly packed network have taken place with the "dissolving" CO_2. Thus, some "hidden" micropores and surface area in the polymers might be accessible for CO_2 to continually permeate into the matrix.[33] The S_{BET} of **PHN-1-TZ** (262 $m^2 g^{-1}$) is much lower than most of reported porous organic polymers[59] such as ACMP-C (629 $m^2 g^{-1}$),[84] CMP-1-COOH (522 $m^2 g^{-1}$),[85] SPOP-7(470 $m^2 g^{-1}$),[86] and COF-102 (3530 $m^2 g^{-1}$).[87] However, the CO_2 uptake capacity of **PHN-1-TZ** can be comparable to, even higher than those materials (6.8 wt% for ACMP-C, 7.0 wt% for CMP-1-COOH, 8.2 wt% for SPOP-7, and 5.3 wt% for COF-102) under the same conditions. From this comparison, the chemical nature changed by post-modification has a crucial influence on the gas uptake capacity of the polymer matrix.

PHN-1-AO and **PHN-2-AO** with amidoxime groups and stable porous structure were performed for uranium adsorption test in simulated seawater with different uranium concentrations (i.e. 10, 20, 30, and 40 ppm) at pH about 7.5. As shown in Fig. 5a, the adsorption capacities of **PHN-1-AO** for uranium at concentrations of 10 and 20 ppm are about 142.5 and 182.7 mg g^{-1}, respectively. When uranium

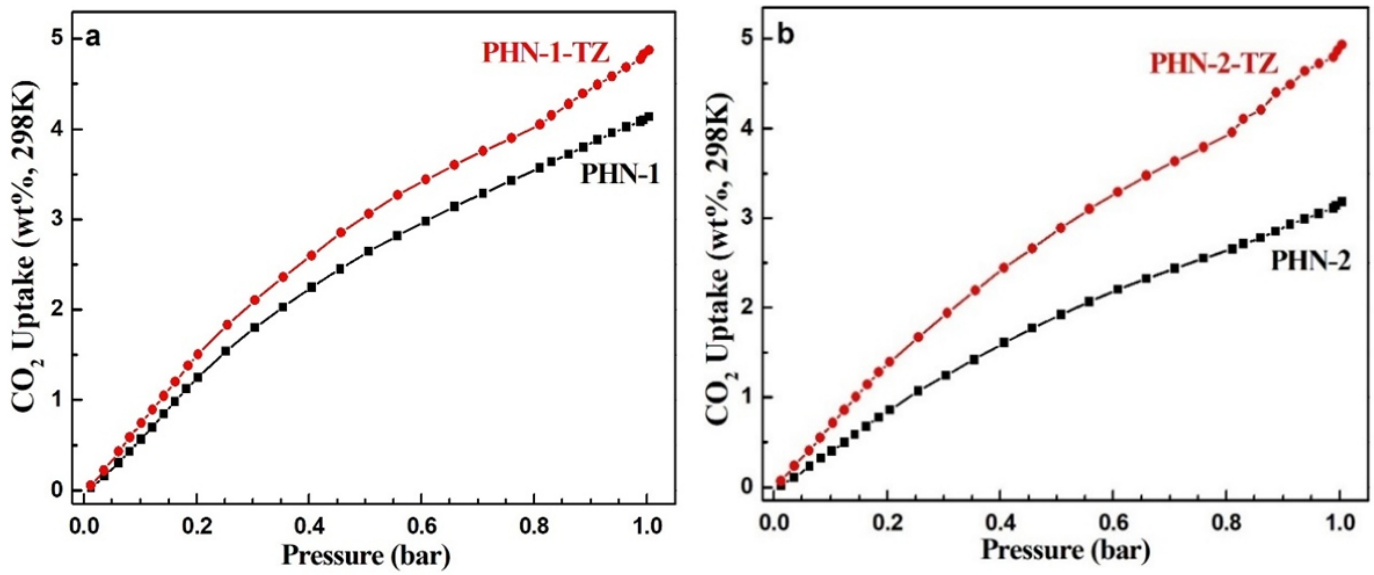

Fig. 4 CO_2 adsorption isotherms of the prepared polymers under the low pressure at 298 K.

© Engineered Science Publisher LLC 2019

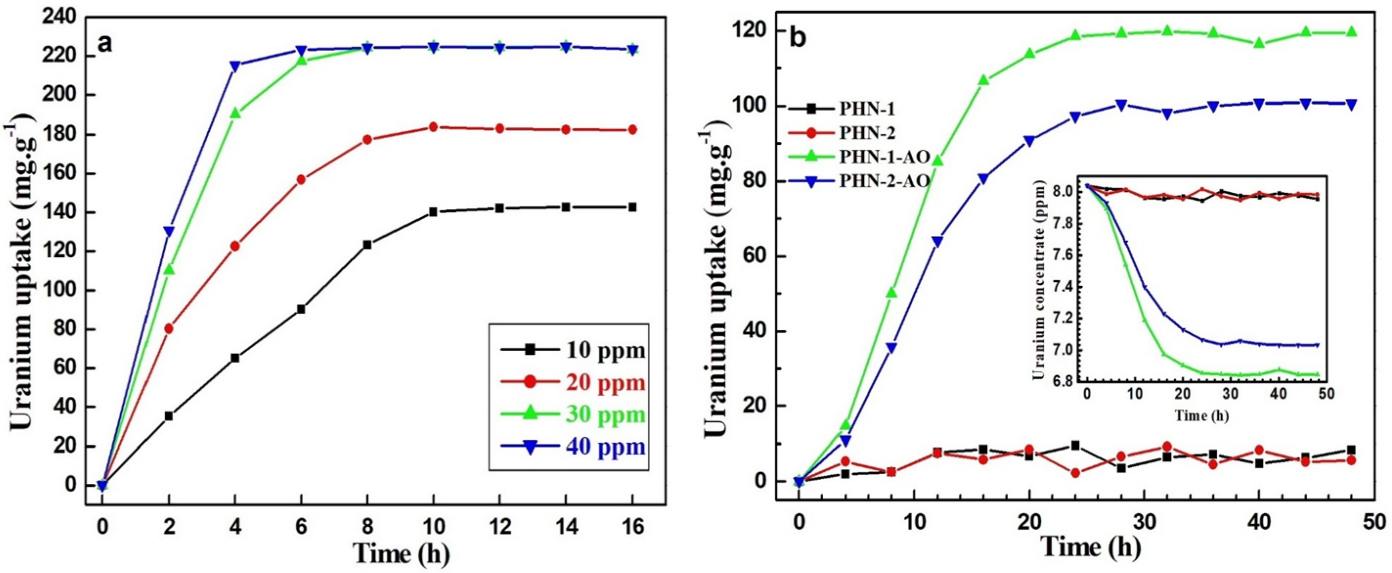

Fig. 5 (a) Uranium adsorption isotherm for **PHN-1-AO** tested in the simulated seawater with different uranium concentrations (10, 20, 30, and 40 ppm) and (b) uranium adsorption isotherm for **PHN-1**, **PHN-2**, **PHN-1-AO**, and **PHN-2-AO** tested in the real seawater with excess uranium (8.02 ppm).

concentration was increased to 30 and 40 ppm, the maximum adsorption capacities of **PHN-1-AO** was about 224.5 mg g^{-1}. Meanwhile, the time required for uptake saturation at lower uranium initial concentration is about 8–10 h, longer than that at higher uranium intial concentration (4–6 h). For **PHN-2-AO**, the maximum adsorption capacity is about 172.4 mg g^{-1} (Fig. S7). As shown in Fig. 5b, further uptake studies in the real seawater with high initial uranium content (8.02 ppm) indicate that the maximum uptake of **PHN-1-AO** (119.4 mg g^{-1}) is higher than that of **PHN-2-AO** (109.2 mg g^{-1}). However, both **PHN-1** and **PHN-2** exhibit inappreciable and unstable uptake capabilities for uranium, implying that the polymers containing amidoxime groups (**PHN-1-AO** and **PHN-2-AO**) by post-modification have significantly enhanced uranium extraction performance. The uranium extration capacity of **PHN-1-AO** in real seawater with excess uranium can be comparable to some reported porous organic polymers, such as PAF-1-CH_2AO (40 mg g^{-1}),[41] MCP (165 mg g^{-1}),[31] and MIPAF-11c (37 mg g^{-1}).[38] After one run of adsorption, **PHN-1-AO** was able to be regenerated for next run of adsorption by treatment with NaOH (1.0 M). As shown in Fig. S8, it is demonstrated that **PHN-1-AO** can keep its uptake capacity for uranium up to three cycles under the same conditions with an adsorption value of 105.6 mg g^{-1}, which is similar to that of the as-prepared **PHN-1-AO** and exhibits the promising economic benefits as the adsorbent for uranium in the seawater.

4. Conclusion

In summary, without using poisonous chemical reagents such as NaCN or CuCN, cyano-containing carbazoles **M-1** and **M-2** were synthesized economically as monomers through the Knoevenagel condensation under the basic condition in 30 mins at room temperature. Oxidative coupling polymerization of **M-1** and **M-2** catalyzed by $FeCl_3$ produced efficiently conjugated polycarbazoles **PHN-1** and **PHN-2** in high yields at room temperature. Cyano groups in the obtained polymers were further transformed to tetrazoles (**PHN-1-TZ** and **PHN-2-TZ**) by treatment with NaN_3/NH_4Cl_3 and amidoxime groups (**PHN-1-AO** and **PHN-2-AO**) by treatment with hydroxylamine aqueous solution, respectively. Chemical structures of polymers were well characterized and comfirmed by FTIR, ^{13}C NMR and XPS measurement. Porosities of all the polymers were evaluated based on their nitrogen adsorption–desorption isotherms at 77 K. The BET specific surface area values of **PHN-1** and **PHN-2** were 340 and 293 m^2 g^1, respectively. Owing to post-modification, porosities of the modified polymers become lower. Post-modification from **PHN-1** and **PHN-2** to the polymers containing tetrazoles (**PHN-1-TZ** and **PHN-2-TZ**) or amidoxime groups (**PHN-1-AO** and **PHN-2-AO**) leads to decreased specific surface areas, which are in the range from 262 to 184 m^2 g^1. Based on the carbon dioxide physisorption isotherms of the related polymers, tetrazole-modified polymers **PHN-1-TZ** and **PHN-2-TZ** with the lower BET specific surface areas exhibit higher CO_2 uptake capacities than corresponding parent polymers, individually. The incorporation of the tetrazole groups into porous polymers has a great promotion on the CO_2 adsorption performance of materials. For example, up to 55.0% enhancement of CO_2 uptake was found for **PHN-2-TZ** (4.93 wt%) after post-modification from **PHN-2** (3.18 wt%) at 298 K and 1.0 bar. The polymers containing amidoxime groups by post-modification have significantly enhanced uranium extraction performance. For example, uranium ion adsorption tests in the real seawater with excess uranium content (8.02 ppm) demonstrates a maximum uptake of 119.4 mg g^{-1} for **PHN-1-AO** whcih is higher than that of **PHN-2-AO** (109.2 mg g^{-1}). However, both **PHN-1** and **PHN-2** exhibit inappreciable and unstable uptake capabilities for uranium ion (about 10 mg g^{-1}). This study demonstrates that the functionalization of cyano-bearing conjugated porous polycarbazoles can remarkably enhance CO_2 uptake, uranium extraction and many other applications.

Acknowledgements

The financial support of the financial support of the Finance Science and Technology Project of Hainan Province (No. ZDYF2018004), the National Natural Science Foundation of China (Grants 51873053, 21574031, 61761016 and 51775152) , and the Start-up Scientific Research Foundation of Hainan University (Grant KYQD(ZR)1812) is acknowledged.

Conflicts of interest

There are no conflicts to declare.

© Engineered Science Publisher LLC 2019

Reference

1. Q. Chen and B. Han, *Macromol. Rapid Commun.,* 2018, **39**, 1800040.
2. R. Dawson, A. Laybourn, R. Clowes, Y. Z. Khimyak, D. J. Adams and A. I. Cooper, *Macromolecules,* 2009, **42**, 8809-8816.
3. X. Liu, Y. Xu and D. Jiang, *J. Am. Chem. Soc*., 2012, **134**, 8738-8741.
4. Q. Chen, M. Luo, P. Hammershøj, D. Zhou, Y. Han, B. W. Laursen, C. Yan and B. Han, *J. Am. Chem. Soc*., 2012, **134**, 6084-6087.
5. X. Zhu, C. Tian, T. Jin, K. L. Browning, R. L. Sacci, G. M. Veith and S. Dai, *ACS Macro Lett*., 2017, **6**, 1056-1059.
6. C. Gu, Y. Chen, Z. Zhang, S. Xue, S. Sun, K. Zhang, C. Zhong, H. Zhang, Y. Pan, Y. Lv, Y. Yang, F. Li, S. Zhang, F. Huang and Y. Ma, *Adv. Mater*., 2013, **25**, 3443-3448.
7. C. Gu, N. Huang, Y. Chen, H. Zhang, S. Zhang, F. Li, Y. Ma and D. Jiang, *Angew. Chem*., *Int. Ed*., 2016, **55**, 3049-3053.
8. A. Palma-Cando and U. Scherf, *ACS Appl. Mater. Inter.,* 2015, **7**, 11127-11133.
9. X. Hu, Z. Salmi, M. Lillethorup, E. B. Pedersen, M. Robert, S. U. Pedersen, T. Skrydstrup and K. Daasbjerg, *Chem. Commun.,* 2016, **52**, 5864-5867.
10. H. Liang, Q. Chen and B. Han, *ACS Catal*., 2018, **8**, 5313-5322.
11. Y. Xu, S. Jin, H. Xu, A. Nagaia and D. Jiang, *Chem. Soc. Rev*., 2013, **42**, 8012-8031.
12. A. Palma-Cando, E. Preis and U. Scherf, *Macromolecules,* 2016, **49**, 8041-8047.
13. S. Hou and B. Tan, *Macromolecules,* 2018, **51**, 2923-2931.
14. X. Li, C. Xu, Z. Chen and H. Wu, *Energy*, 2011, **36**, 1394-1403.
15. D. Cui, C. Yao and Y. Xu, *Chem. Commun*., 2017, **53**, 11422-11425.
16. X. Li, C. Xu, Z. Chen and H. Wu, *Energy*, 2010, **35**, 3902-3908.
17. Y. Liao, Z. Cheng, W. Zuo, A. Thomas and C. F. J. Faul, *ACS Appl. Mater. Inter.,* 2017, **9**, 38390-38400.
18. D. Yuan, W. Lu, D. Zhao and H. Zhou, *Adv. Mater*., 2011, **23**, 3723-3725.
19. X. Li, H. Zhan, C. Xu, Z. Zeng, Q. Lv and K. Yan, *Energy Fuel.*, 2012, **26**, 2518-2527.
20. L. Tang, X. Li, Z. Feng, G. Li and S. Fan, *Energy Fuel.,* 2007, **21**, 227-233.
21. G. Li, G. J. Moridis, K. Zhang and X. Li, *Energy Fuel.*, 2010, **24**, 6018-6033.
22. X. Li, B. Yang, Y. Zhang, G. Li, L. Duan, Y. Wang, Z. Chen, N. Huang and H. Wu, *Appl. Energy*, 2012, **93**, 722-732.
23. B. Li, X. Li, G. Li, J. Feng and Y. Wang, *Appl. Energy*, 2014, **129**, 274-286.
24. G. Li, X. Li, L. Tang and Y. Zhang, *Energy Fuel.,* 2007, **21**, 3388-3393.
25. D. M. D'Alessandro, B. Smit and J. R. Long, *Angew. Chem*., *Int. Ed*., 2010, **49**, 6058-6082.
26. X. Li, Z. Xia, Z. Chen, K. Yan, G. Li and H. Wu, *J. Chem. Eng. Data*, 2010, **55**, 2180-2184.
27. X. Li, C. Xu, Z. Chen and J. Cai, *Int. J. Hyderogen. Energ*., 2012, **37**, 720-727.
28. S. Chu and A. Majumdar, *Nature,* 2012, **488**, 294-303.
29. D. S. Sholl, R. P. Lively, *Nature,* 2016, **532**, 435-438.
30. C. Hou, Y. Hou, Y. Fan, Y. Zhai, Y. Wang, Z. Sun, R. Fan, F. Dang and J. Wang, *J. Mater. Chem. A,* 2018, **6**, 6967-6976.
31. B. He, J. Wang, Y. Fan, Y. Jiang, Y. Zhai, Y. Wang, Q. Huang, N. Wang, F. Dang and Z. Zhang, *J. Mater. Chem. A*, 2018, **6**, 19075-19084.
32. C. Hou, Z. Tai, L. Zhao, Y. Zhai, Y. Hou, Y. Fan, F. Dang, J. Wang and H. Liu, *J. Mater. Chem. A*, 2018, **6**, 9723-9736.
33. Q. Chen, D. Liu; M. Luo, L. Feng, Y. Zhao and B. Han, *Small,* 2014, **10**, 308-315.
34. Q. Chen, D. Liu, J. Zhu and B. Han, *Macromolecules,* 2014, **47**, 5926-5931.
35. T. Jin, Y. Xiong, X. Zhu, Z. Tian, D. Tao, J. Hu, D. Jiang, H. Wang, H. Liu and S. Dai, *Chem. Commun*., 2016, **52**, 4454-4457.
36. F. Jiang, T. Jin, X. Zhu, Z. Tian, C. Do-Thanh, J. Hu, D. Jiang, H. Wang, H. Liu and S. Dai, *Macromolecules,* 2016, **49**, 5325-5330.
37. Y. Fu, Z. Wang, X. Fu, J. Yan, C. Liu, C. Pan and G. Yu, *J. Mater. Chem. A,* 2017, **5**, 21266-21274.
38. Y. Yue, R. T. Mayes, J. Kim, P. F. Fulvio, X. Sun, C. Tsouris, J. Chen, S. Brown and S. Dai, *Angew. Chem*., *Int. Ed*., 2013, **52**, 13458-13458.
39. C. W. Abney, R. T. Mayes, T. Saito and S. Dai, *Chem. Rev*., 2017, **117**, 13935-14013.
40. D. Wang, J. Song, J. Wen, Y. Yuan, Z. Liu, S. Lin, H. Wang, H. Wang, S. Zhao, X. Zhao, M. Fang, M. Lei, B. Li, N. Wang, X. Wang and H. Wu, *Adv. Energy Mater*., 2018, **8**, 1802607.
41. B. Li, Q. Sun, Y. Zhang, C. W. Abney, B. Aguila, W. Lin and S. Ma, *ACS Appl. Mater. Inter.,* 2017, **9**, 12511-12517.
42. Y. Qian, Y. Yuan, H. Wang, H. Liu, J. Zhang, S. Shi, Z. Guo and N. Wang, *J. Mater. Chem. A,* 2018, **6**, 24676-24685.
43. W. Luo, G. Xiao, F. Tiane, J. J. Richardson, Y. Wang, J. Zhou, J. Guo, X. Liao and B. Shi, *Energy Environ. Sci.,* 2019, **12**, 607-614.
44. C. Liu, P. Hsu, J. Xie, J. Zhao, T. Wu, H. Wang, W. Liu, J. Zhang, S. Chu and Y. Cui, *Nat. Energy,* 2017, **2**, 17007.
45. R. V. Davies, J. Kennedy, R. W. McIlroy, R. Spence and K. M. Hill, *Nature*, 1964, **203**, 1110-1115.
46. Y. Yuan, S. Zhao, J. Wen, D. Wang, X. Guo, L. Xu, X. Wang and N. Wang, *Adv. Funct. Mater.,* 2019, **29**, 1805380.
47. E. Macerata, E. Mossini, S. Scaravaggi, M. Mariani, A. Mele, W. Panzeri, N. Boubals, L. Berthon, M. Charbonnel, F. Sansone, A. Arduini and A. Casnati, *J. Am. Chem. Soc*., 2016, **138**, 7232-7235.
48. Y. Yue, C. Zhang, Q. Tang, R. T. Mayes, W. Liao, C. Liao, C. Tsouris, J. J. Stankovich, J. Chen, D. K. Hensley, C. W. Abney, D. Jiang, S. Brown and S. Dai, *Ind. Eng. Chem. Res*., 2016, **55**, 4125-4129.
49. X. Han, M. Xu, S. Yang, J. Qian and D. Hua, *J. Mater. Chem. A,* 2017, **5**, 5123-5128.
50. L. Chen, Z. Bai, L. Zhu, L. Zhang, Y. Cai, Y. Li, W. Liu, Y. Wang, L. Chen, J. Diwu, J. Wang, Z. Chai and S. Wang, *ACS Appl. Mater. Inter.,* 2017, **9**, 32446-32451.
51. Z. Bai, L. Yuan, L. Zhu, Z. Liu, S. Chu, L. Zheng, J. Zhang, Z. Chai and W. Shi, *J. Mater. Chem. A,* 2015, **3**, 525-534.
52. L. Li, W. Ma, S. Shen, H. Huang, Y. Bai and H. Liu, *ACS Appl. Mater. Inter.,* 2016, **8**, 31032-31041.
53. Y. Yuan, Y. Yang, X. Ma, Q. Meng, L. Wang, S. Zhao and G. Zhu, *Adv. Mater*., 2018, **30**, 1706507.
54. C. Gunathilake, J. G´orka, S. Dai and M. Jaroniec, *J. Mater. Chem. A,* 2015, **3**, 11650-11659.
55. L. Ling and W. Zhang, *J. Am. Chem. Soc*., 2015, **137**, 2788-2791.
56. Q. Sun, B. Aguila, J. Perman, A. S. Ivanov, V. S. Bryantsev, L. D. Earl, C. W. Abney, L. Wojtas and S. Ma, *Nat. Commun*., 2018, **9**, 1644.
57. Q. Sun, B. Aguila, L. D. Earl, C. W. Abney, L. Wojtas, P. K. Thallapally and S. Ma, *Adv. Mater*., 2018, **30**, 1705479.
58. A. Palma-Cando, D. Woitassek, G. Brunklaus and U. Scherf, *Mater. Chem. Front*., 2017, **1**, 1118-1124.
59. Q. Chao, Q. Yin, Q. Chen, Z. Dong and B. Han, *Chem. Eur. J.* 2017, **23**, 9831-9837.
60. L. Feng, Q. Chen, J. Zhu, D. Liu, Y. Zhao and B. Han, *Polym. Chem*., 2014, **5**, 3081-3088.
61. S. Das, P. Heasman, T. Ben and S. Qiu, *Chem. Rev*., 2016, **117**, 1515-1563.
62. L. Pan, M. Xu, L. Feng, Q. Chen, Y. He and B. Han, *Polym. Chem*., 2016, **7**, 2299-2307.
63. S. Lee, G. Barin, C. M. Ackerman, A. Muchenditsi, J. Xu, J. A. Reimer, S. Lutsenko, J. R. Long and C. J. Chang, *J. Am. Chem. Soc.,* 2016, **138**, 7603-7609.
64. S. Ding, C. Tian, X. Zhu, C. W. Abney, Z. Tian, B. Chen, M. Li, D. Jiang, N. Zhang and S. Dai, *Chem. Sus. Chem,* 2017, **10**, 2348-2351.
65. B. Hu, X. Zhu, S. Peng, X. Chen, L. Pan, Q. Yan and R. Li, *J. Mater. Chem.* 2012, **22**, 520-526.
66. G. Jones, *Org. React. N. Y*., 1967, **15**, 204-599.
67. Y. Wei, W. Chen, X. Zhao, S. Ding, S. Han and L. Chen, *Polym. Chem*., 2016, **7**, 3983.
68. K. Zhang, D. Kopetzki, P. H. Seeberger, M. Antonietti and F. Vilela, *Angew. Chem., Int. Ed.*, 2013, **52**, 1432-1436.
69. J. Zhu, Q. Chen, Z. Sui, L. Pan, J. Yu and B. Han, *J. Mater. Chem. A*, 2014, **2**, 16181-16189.
70. J. Luo, X. Zhang, J. Lu and J. Zhang, *ACS Catal.*, 2017, **7**, 5062-5070.
71. L. Pan, Q. Chen, J. Zhu, J. Yu, Y. He and B. Han, *Polym. Chem.*, 2015, **6**, 2478-2487.
72. C. Xu and N. Hedin, *Mater. Today*, 2014, **17**, 397-403.
73. R. Zhang, Q. Yin, H. Liang, Q. Chen, W. Luo and B. Han, *Polymer*, 2018, **143**, 87-95.
74. N. Du, H. B. Park, G. P. Robertson, M. M. Dal-Cin, T. Visser, L. Scoles and

© Engineered Science Publisher LLC 2019

M. Guiver, *Nat. Mater*., 2011, **10**, 372-375.
75. Y. Zhang, Y. Chen, C. Wang and Y. Wei, *J. Hazard. Mater*., 2014, **276**, 129-137.
76. B. Yan, X. Du, R. Huang, J. Yang, Z. Wang, S. Zang and T. C. W. Mak, *Inorg. Chem.,* 2018, **57**, 4828.
77. A. Dong, T. Dai, M. Ren, X. Zhao, S. Zhao, Y. Yuan, Q. Chen and N. Wang, *Eng. Sci.,* 2019, **5**, 56-65.
78. K. S. Sing, D. H. Everett, R. A. W. Haul, L. Moscou, R. A. Pierotti, J. Rouquérol and T. Siemieniewska, *Pure Appl. Chem*., 1985, **57**, 603-619.
79. B. Li, Z. Guan, W. Wang, X. Yang, J. Hu, B. Tan and T. Li, *Adv. Mater*. 2012, **24**, 3390-3395.
80. A. Dong, D. Wang, T. Dai, Q. Chen, L. Feng and N. Wang, *Adv. Compos. Hybrid Mater.,* 2018, **1**, 696-704.
81. C. Xu, S. Zhang, J. Cai, Z. Chen and X. Li, *Energy*, 2013, **59**, 719-725.
82. X. Li, Z. Xia, Z. Chen and H. Wu, *Energy Fuel*., 2011, **25**, 1302-1309.
83. X. Li, Y. Liu, Z. Zeng, Z. Chen, G. Li and H. Wu, *J. Chem. Eng. Data*, 2011, **56**, 119–123.
84. J. H. Choi, K. J. Choi, H. J. Jeon, Y. J. Choi, Y. Lee and J. K. Kang, *Macromolecules,* 2010, **43**, 5508-5511.
85. R. Dawson, D. J. Adams and A. I. Cooper, *Chem. Sci.,* 2011, **2**, 1173-1177.
86. M. Jiang, Q. Wang, Q. Chen, X. Hu, X. Ren, Z. Li and B. Han, *Polymer,* 2013, **54**, 2952-2957.
87. H. Furukawa and O. M. Yaghi, *J. Am. Chem. Soc.,* 2009, **131**, 8875-8883.

Publisher's Note Engineered Science Publisher remains neutral with regard to jurisdictional claims in published maps and institutional affiliations.

 © Engineered Science Publisher LLC 2019